Chemical tools to modulate endocannabinoid biosynthesis

Deng, H.

8

Summary and future prospects

In **Chapter 1**, the endocannabinoid system is introduced. Endocannabinoids are endogenous signaling lipids that activate cannabinoid CB_1 and CB_2 receptors.[1,2] Endocannabinoids can be considered as the body's own marijuana, because CB receptors are also targeted by Δ^9-tetrahydrocannabinol, the psychoactive principle of marijuana.[3] Endocannabinoids play an essential role in human health and disease, regulating processes, such as immunomodulation, energy balance, neurotransmission, mood, appetite, pain sensation and reward.[4-9] Endocannabinoids are also involved in pathophysiological conditions. Continuous stimulation of the CB_1 receptor by endocannabinoids is associated with nicotine addiction, obesity and the metabolic syndrome (all major risk factors for illness and death in Europe).[8] The CB_1 receptor blocker Rimonabant was effective in obese patients, but was withdrawn from the European market due to unacceptable psychiatric side effects (i.e. depression, anxiety and suicidal ideation in some individuals).[10,11] This highlights the medical need to modulate the endocannabinoid system in a more controlled manner.

There are two main endocannabinoids: anandamide and 2-arachidonoylglycerol (2-AG).[12] Both endocannabinoids have an arachidonic acid backbone, but vary in their polar head group. Both endocannabinoids are often found together, but their levels vary between species, tissue, developmental stage and pathological condition. Although, selective inhibitors of their metabolic pathways have provided information about the biological function of the endocannabinoids, it is still unclear to a large extent which endocannabinoid is responsible for specific cannabinoid CB_1 and CB_2 receptor dependent (patho)physiological effects.[13] Selective inhibition of the formation of anandamide and 2-AG would be instrumental to determine which endocannabinoid is responsible for specific CB_1-mediated physiological effects. However, pathway-selective and *in vivo* active inhibitors for 2-AG and anandamide biosynthesis are currently lacking.

Endocannabinoids are produced “on demand” upon different biological stimuli via different biosynthetic pathways. 2-AG is mainly formed by the action of two diacylglycerol lipases (DAGL-α and DAGL-β).[14] Studies with DAGL-KO mice have shown that DAGL-α controls to a large extent the formation of 2-AG in the central nervous system, whereas DAGL-β appears to partake in 2-AG production in the periphery (Table 1).[15-17] Selective DAGL-α inhibition has been hypothesized to be an alternative for Rimonabant, whereas selective DAGL-β inhibitors are envisioned to have protective properties by reducing neuroinflammation.[18]

Table 1. Reductions of 2-AG levels in DAGL$\alpha^{-/-}$ and DAGL$\beta^{-/-}$ mouse tissues.

	DAGL$\alpha^{-/-}$	DAGL$\beta^{-/-}$
Brain	~80%	~50%
Spinal cord	~80%	0%
Liver	~60%	~90%
Adipose	~50%	0%

The discovery of DAGL inhibitors has, however, been hindered by a lack of DAGL crystal structures and a dearth of functional assays to evaluate endogenous DAGL activity. Currently, several classes of DAGL inhibitors have been discovered. Among them are bis-oximino-carbamates (RHC-80267), β-lactones (THL) and fluorophosphonates (MAFP, O-3640, O-3841 and O-5596), which are the first-generation of covalent (ir)reversible DAGL inhibitors.[19,20] Most of these inhibitors are lipid-based molecules that are not selective over other lipases and/or lack *in vivo* activity on DAGL. In 2012, the triazole ureas KT109 and KT172 were reported as the first specific and *in vivo* active DAGLβ inhibitors.[18] Hsu *et al.* discovered that inhibition of DAGLβ reduced 2-arachidonolyglycerol (2-AG), arachidonic acid and eicosanoids levels in peritoneal macrophages of lipopolysaccharide (LPS)-treated mice and significantly decreased pro-inflammatory cytokines.[18] Yet, these inhibitors were not

brain-penetrable and did not inhibit DAGLα, thus, the main aim of this thesis was to develop highly selective and *in vivo* CNS-active DAGL inhibitors to study DAGL function in the brain.

In **Chapter 2** the enantioselective synthesis and structure-activity-relationship (SAR) studies of 2,4-regioisomer of 1,2,3-triazole ureas as a novel chemotype of DAGLα inhibitors is described. It was found that (*R*)-benzylpiperidine substituted triazole ureas constitute the active enantiomer for DAGLα inhibition as measured in biochemical assays and activity-based protein profiling. It was shown that (*R*)-KT109 was the eutomer. The investigations culminated in the discovery of DH376, as a highly potent, cellular active DAGL inhibitor.

In **Chapter 3**, DAGL inhibitors DH376 and DO34 (Figure 1) as well as a structurally related control compound DO53 (see structure in Chapter 3) were further characterized and used, in combination with chemical proteomics and lipidomics, to determine the impact of acute DAGL blockade on brain lipid networks in mice. Within two hours, DAGL inhibition produced a striking reorganization of bioactive lipids, including elevations in DAGs and reductions in endocannabinoids and eicosanoids. It was also found that DAGLα is a short half-life protein, and the inactivation of DAGLs disrupts cannabinoid receptor-dependent synaptic plasticity and impairs neuroinflammatory responses, including lipopolysaccharide-induced anapyrexia. These findings illuminated the highly interconnected and dynamic nature of lipid signaling pathways in the brain and the central role that DAGL enzymes play in regulating this network.

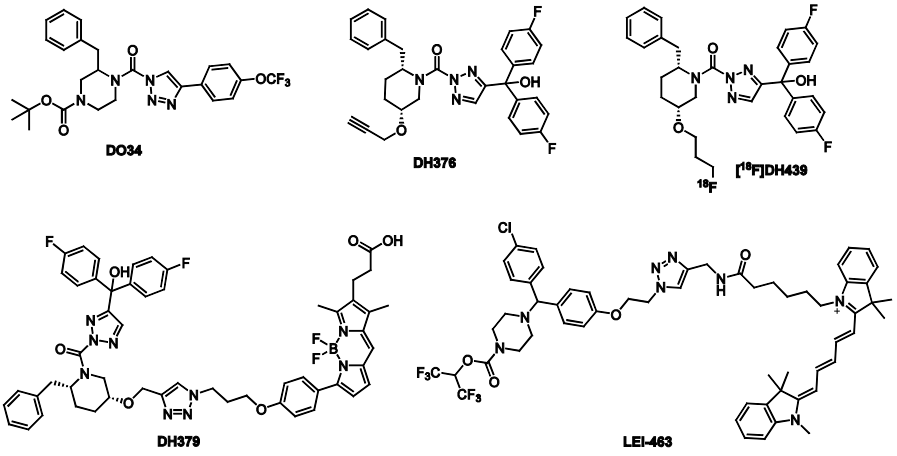

Figure 1. Structures of chemical probes described in the thesis. DO34 and DH376 are *in vivo* CNS-active DAGL inhibitors; [^{18}F]DH439 is a potential PET tracer candidate for DAGL; LEI-463 is a highly selective and potent activity-based imaging probe for MAGL.

In **Chapter 4** the therapeutic efficacy of DAGL inhibitors as a potential anti-obesity treatment was investigated.[17,21] DH376 temporarily reduced fasting-induced refeeding of mice, emulating the effects of cannabinoid CB_1-receptor inverse agonists. As a consequence of reduced food intake, increased fat oxidation and lowered carbohydrate metabolism was observed in DH376-treated mice. Moreover, DH376 did not affect locomotion. These effects were mirrored by DO34, but also by negative control compound DO53, which indicated that the triazole ureas may affect the energy balance in mice through multiple molecular targets. Further selectivity studies were performed to assess the selectivity profile of DH376 in peripheral tissues.

In **Chapter 5**, the design, synthesis and application of [^{18}F]DH439 as a positron emission tracer for DAGL is described. Activity-based protein profiling (ABPP) and radioligand displacement assays demonstrated that DH439 maintained good potency and selectivity against DAGLs, but did show some affinity towards CB_2 receptor. Biodistribution and PET-imaging experiments using [^{18}F]DH439 in mice showed good uptake in peripheral tissues, but low tracer uptake in the brain.

To improve physico-chemical properties of triazole ureas, the structure-activity-relationship of triazole ureas featuring chiral, hydroxylated disubstituted piperidines as dual inhibitors of DAGLα and ABHD6 were investigated in **Chapter 6**. The chirality of the carbon bearing the C2 substituent, as well as the position of the hydroxyl (tolerated at C5, but not at C3) had profound influence on the inhibitory activity of both DAGLα and ABHD6, as established using biochemical assays and competitive activity-based protein profiling on mouse brain extracts (Figure 2). Inhibition of ABHD6 has been reported to produce neuroprotective, anti-obesity and anti-inflammatory effects in preclinical disease models.[22,23] Thus, dual inhibitors of DAGLs and ABHD6 are potential leads for the development of therapeutic agents for metabolic and neurodegenerative disorders.

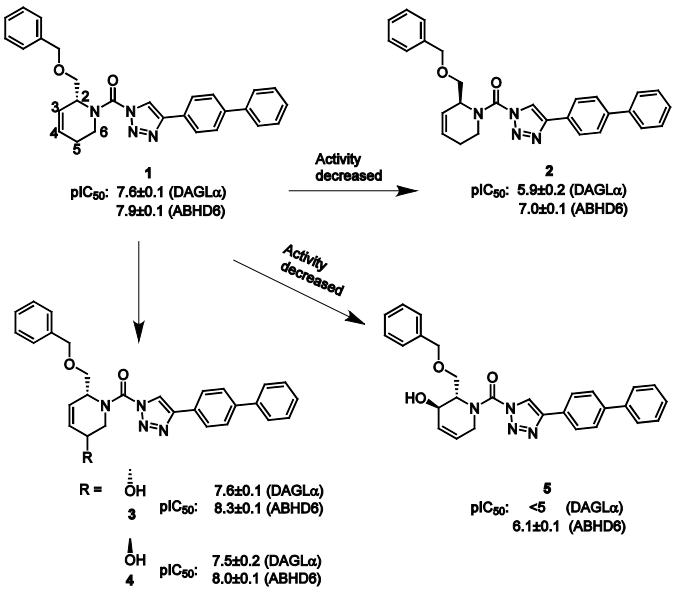

Figure 2. Structure-activity relationships (SAR) of disubstituted piperidinylureas as dual inhibitors of DAGLα and ABHD6.

Monoacylglycerol lipase (MAGL) activity is tightly regulated in both normal and disease conditions. For example, MAGL is highly expressed in aggressive human cancer cells and primary tumors, where it regulates a set of pro-tumorigenic signals.[24] Specific chemical probes that target MAGL are required to monitor the dynamic nature of lipid signaling in living cells or whole organism, but are currently not available. To address this limitation, a potent, selective and cell-permeable activity-based probe LEI-463 (Figure 1) was developed in **Chapter 7**. LEI-463 showed high selectivity over other serine hydrolases, including ABHD6, a common off-target for most MAGL inhibitors and probes. LEI-463 was used to visualize MAGL activity in MCF7 cells by fluorescence confocal microscopy and correlative light electron microscopy. Mitochondria were identified as the principle subcellular compartment where MAGL resides. It is envisioned that LEI463 may serve as a valuable tailored ABP to study MAGL activity and distribution during (patho)physiological processes and may serve as a biomarker for target engagement studies to guide drug development.

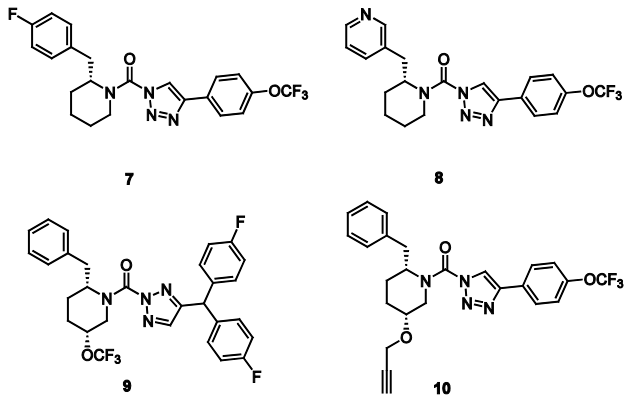

Figure 3. Proposed DAGLs inhibitors for improving pharmacokinetic properties.

Future prospects

In this thesis, a set of chemical probes is described to modulate and visualize 2-AG production via acute inhibition of DAGLs. These chemical probes are not specific for each isoform, therefore the development of inhibitors that can selectively inhibit DAGLα or DAGLβ would be of value to investigate the physiological roles of each isoform.Since high doses (50 mg/kg, i.p.) are required to maintain complete target engagement over a prolonged period of time (> 8 h), improvement of the pharmacokinetic properties of DH376 is desired to lower the effective dose required for *in vivo* studies. There are multiple possibilities to improve the pharmacokinetic properties of the DAGL inhibitors. In general, the lipophilicity of the inhibitors should be further reduced and metabolite identification could be performed to identify metabolic hot spots. Potential metabolic sites may include the propargylether, the benzylic position of the 2-benzylpiperidine and the para-position on the phenyl ring of DH376. It is envisioned that compounds **7-9** and hybrid molecules of DH376 and DO34 (e.g. (**10**)) may represent selective DAGL inhibitors with improved physicochemical properties and improved metabolic stability. DH376 is a substrate of the PgP-transporter (unpublished data), therefore the number of H-bond donors and acceptors should be lowered to reduce its interaction with the transporter protein and to improve its brain penetration. These new compounds may also serve as leads for the development of new PET tracers for in vivo target engagement studies.

In sharp contrast to the 2-AG biosynthetic pathway, the biosynthesis of the other endocannabinoid anandamide is still poorly understood due to the lack of molecular tools to modulate and detect the proteins responsible for anandamide biosynthesis. Anandamide belongs to the class of *N*-acylethanolamines (NAEs), which is an important family of bioactive lipids in the central nervous system.[1,2] A calcium-dependent *N*-acyltransferase (NAT) that generates *N*-acyl

phosphatidylethanolamines (NAPEs) is the rate-limiting step in the biosynthesis of NAEs in the brain.[12,25,26] Recently, the poorly characterized serine hydrolase PLA2G4E was discovered to act as a mouse brain Ca^{2+}-dependent NAT by Ogura *et. al*.[27] They showed that this enzyme generates NAPEs and NAEs in mammalian cells. Thus, PLA2G4E is an interesting target to modulate and study the *in vivo* functions of NAPEs and NAEs, including anandamide. To this end, potent and selective PLA2G4E inhibitors and activity-based probes are required.

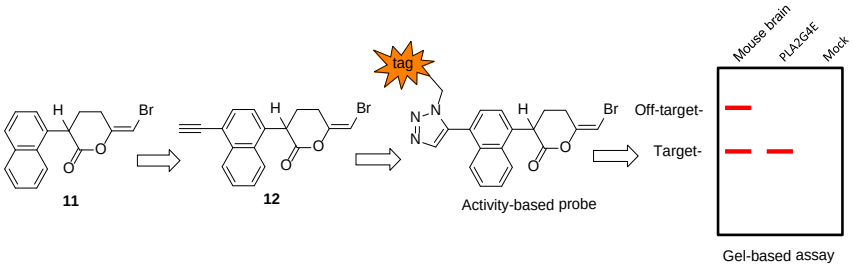

Figure 4. Proposed strategy to design and identify activity-based probe for PLA2G4E.

Previously, (*E*)-6-(bromomethylene)-3-(naphthalen-1-yl)tetrahydro-*2H*-pyran-2-one (**11**) (Figure 4) has been shown to non-selectively covalently inhibit NAT activity with an IC_{50} of 2 µM.[28] Compound **11** may, therefore, represent as an excellent starting point for the development of PLA2G4E inhibitors and activity-based probes. An alkyne or azide can be introduced at various positions of the naphtyl moiety to serve as a ligation handle to introduce fluorophores or a biotin. As an example, probe **12** (Figure 4) was synthesized according to the route depicted in Scheme 1. Subsequent introduction of a fluorescent reporter tag by copper-catalyzed azide-alkyne cycloaddition (CuAAC, or "click") chemistry generated a direct activity-based probe **13** for future target engagement studies of PLA2G4E. To validate the activity of probe **13** against PLA2G4E, gel-based ABPP assay with recombinant PLA2G4E (using Mock as a negative control) or mouse brain proteome should be performed.

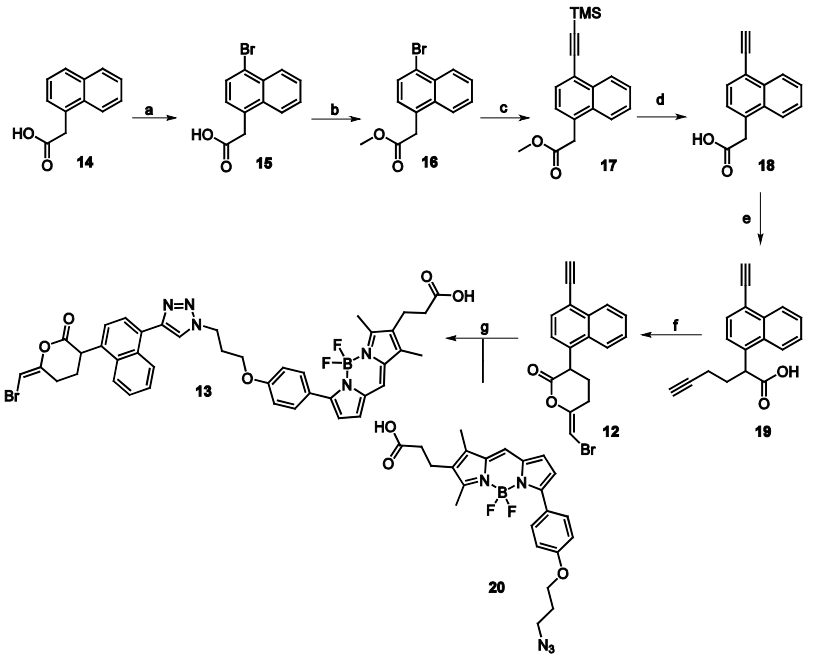

Scheme 1. Synthesis route of proposed activity-based probe for PLA2G4E. Reagents and conditions: (a) Br_2, AcOH, 50-60 ^{o}C, 50%; (b) MeOH, H_2SO_4, 65 ^{o}C, 95%; (c) Ethynyltrimethylsilane, triethylamine, CuI, $PdCl_2(PPh_3)_2$, DMF:1,4-dioxane (1:2.5), reflux, 31%; (d) LiOH, MeOH:H_2O (3:1), r.t., 73%; (e) 4-Bromobut-1-yne, LDA, HMPA, THF, -20 ^{o}C, 62%; (f) NBS, $KHCO_3$, H_2O, DCM, r.t., 8%; (g) $CuSO_4$, sodium ascorbate, DCM/H_2O (1:1), r.t., 38%.

Experimental section

Chemistry

General materials: All of reactions were performed using oven or flame-dried glassware and dry solvents. Reagents were purchased from Sigma Aldrich, Acros and Merck and used without further purification unless noted otherwise. All moisture sensitive reactions were performed under an argon atmosphere. Traces of water were removed from starting compounds by co-evaporation with toluene. ^{1}H-and ^{13}C-NMR spectra were recorded on a Bruker AV 400 MHz spectrometer at 400 (^{1}H) and 101 (^{13}C) MHz, or on a Bruker DMX-600 spectrometer 600 (^{1}H) and 150 (^{13}C) MHz using $CDCl_3$, or CD_3OD solvent, unless stated otherwise. Chemical shift values are reported in ppm with tetramethylsilane or solvent resonance as the internal standard ($CDCl_3$, δ 7.26 for ^{1}H, δ 77.16 for ^{13}C; CD_3OD, δ 3.31 for ^{1}H, δ 49.00 for ^{13}C). Data are reported as follows: chemical shifts (δ), multiplicity (s = singlet, d = doublet, dd = double doublet, td = triple doublet, t = triplet, m = multiplet, br = broad), coupling constants *J*

(Hz), and integration. High-resolution mass spectra (HRMS) were recorded by direct injection (2 µL of a 2 µM solution in water/acetonitrile 50/50 (v/v) and 0.1% formic acid) on a mass spectrometer (Thermo Finnigan LTQ orbitrap) equipped with an electrospray ion source in positive mode (source voltage 3.5 kV, sheath gas flow 10, capillary temperature 250 ^{o}C) with resolution R = 60,000 at m/z 400 (mass range m/z = 150-2,000) and dioctylphthalate (m/z = 391.28428) as a "lock mass". The high resolution mass spectrometer was calibrated prior to measurements with a calibration mixture (Thermo Finnigan). LC-MS analysis was performed on a Finnigan Surveyor HPLC system with a Gemmi C_{18} 50x4.60 mm column (detection at 200-600 nm), coupled to a Finnigan LCQ Adantage Max mass spectrometer with ESI. The applied buffers were H_2O, MeCN and 1.0% TFA in H_2O (0.1% TFA end concentration). Flash chromatography was performed using SiliCycle silica gel type SilicaFlash P60 (230 – 400 mesh). TLC analysis was performed on Merck silica gel 60/Kieselguhr F254, 0.25 mm. Compounds were visualized using either Seebach's reagent (a mixture of phosphomolybdic acid (25 g), cerium (IV) sulfate (7.5 g), H_2O (500 mL) and H_2SO_4 (25 mL)) or a $KMnO_4$ stain (K_2CO_3 (40 g), $KMnO_4$ (6 g), H_2O (600 mL) and 10% NaOH (5 mL)).

2-(4-Bromonaphthalen-1-yl)acetic acid (15). A solution of compound **14** (6.0 g, 32 mmol) in 3mL glacial acetic acid was added bromine (1.63 mL, 31.6 mmol) dropwise with stirring, and then the mixture was heated at 50-60 ^{o}C for 2h. After that the mixture was allowed to stand at 20 ^{o}C for 6h, the resulting precipitate was collected by filtration and washed with aqueous acetic acid to afford the crude product that was recrystallized from chloroform to afford pure product (4.24 g, 15.99 mmol, 50% yield). ^{1}H NMR (400 MHz, $CDCl_3$) δ 8.34 – 8.23 (m, 1H), 7.94 (dd, *J* = 7.3, 1.9 Hz, 1H), 7.74 (d, *J* = 7.6 Hz, 1H), 7.65 – 7.55 (m, 2H), 7.29 – 7.19 (m, 1H), 4.05 (s, 2H). ^{13}C NMR (101 MHz, $CDCl_3$) δ 176.98, 133.28, 132.29, 129.96, 129.68, 128.70, 128.22, 127.50, 127.46, 124.29, 123.25, 38.70.

Methyl 2-(4-bromonaphthalen-1-yl)acetate (16) A solution of compound **15** (4.2 g, 15.8 mmol) in MeOH and sulfuric acid (5.91 mL, 111 mmol) was heated at reflux overnight. The reaction mixture was concentrated and extracted with EtOAc and $NaHCO_3$, washed with water, brine and dried over $MgSO_4$, filter. After concentration under reduced pressure, the residue was purified by silica gel chromatography (pentane/ EtOAc = 1%-10%) to afford title compound (4.2 g, 15 mmol, 95% yield). ^{1}H NMR (400 MHz, $CDCl_3$) δ 8.20 – 8.13 (m, 1H), 7.87 – 7.77 (m, 1H), 7.57 (d, *J* = 7.6 Hz, 1H), 7.48 – 7.39 (m, 2H), 7.04 (d, *J* = 7.6 Hz, 1H), 3.85 (s, 2H), 3.53 (s, 3H). ^{13}C NMR (101 MHz, $CDCl_3$) δ 171.11, 132.96, 131.77, 130.46, 129.28, 128.09, 127.60, 126.94, 126.93, 124.02, 122.41, 51.90, 38.45.

Methyl 2-(4-((trimethylsilyl)ethynyl)naphthalen-1-yl)acetate (17). To a solution of ethynyltrimethylsilane (1.82 mL, 12.9 mmol), compound **16** (1.80 g, 6.45 mmol), $PdCl_2(PPh_3)_2$ (679 mg, 0.97 mmol) and CuI (184 mg, 0.97 mmol) were suspended in the mixture of dry DMF (20 mL), 1,4-dioxane (8.0 mL) and triethylamine (9.0 mL, 64.5 mmol). The mixture was refluxed for 24h, and then diluted with DCM, washed with

brine, water, dried over $MgSO_4$ and filtered. After concentration, the residue was purified by silica gel chromatography (pentane/Et_2O = 1%-10%) to afford title compound (600 mg, 2.02 mmol, 31% yield). ^{1}H NMR (400 MHz, $CDCl_3$) δ 8.51 (d, *J* = 8.0 Hz, 1H), 8.04 (d, *J* = 7.7 Hz, 1H), 7.74 (d, *J* = 7.9 Hz, 1H), 7.71 – 7.56 (m, 2H), 7.37 (d, *J* = 7.3 Hz, 1H), 4.09 (s, 2H), 3.71 (s, 3H), 0.45 (s, 9H). ^{13}C NMR (101 MHz, $CDCl_3$) δ 171.52, 133.64, 131.78, 131.71, 130.40, 127.37, 127.01, 126.88, 126.71, 124.08, 120.78, 103.25, 99.66, 52.10, 39.06, 0.16.

2-(4-Ethynylnaphthalen-1-yl)acetic acid (18). Compound **17** (200 mg, 0.675 mmol) was dissolved in a mixture of MeOH-H_2O (3:1, 4 mL), and LiOH (22.62 mg, 0.945 mmol) was added. After 20h at room temperature, the reaction mixture was concentrated, diluted with water and acidified with concentrated HCl to pH4. The resultant mixture was extracted with ethyl acetate (3 X 20 mL), the combined extracts dried over $MgSO_4$, and the solvent was evaporated to give the crude acid without further purification (104 mg, 0.495 mmol, 73% yield). ^{1}H NMR (400 MHz, $CDCl_3$) δ 9.95 (br, 1H), 8.52 – 8.39 (m, 1H), 8.05 – 7.91 (m, 1H), 7.69 (d, *J* = 7.3 Hz, 1H), 7.64 – 7.49 (m, 2H), 7.36 (d, *J* = 7.3 Hz, 1H), 4.08 (s, 2H), 3.49 (s, 1H). ^{13}C NMR (101 MHz, $CDCl_3$) δ 177.48, 133.89, 131.84, 131.34, 130.91, 127.66, 127.22, 127.08, 127.03, 124.15, 120.27, 82.46, 81.73, 38.99.

2-(4-Ethynylnaphthalen-1-yl)hex-5-ynoic acid (19). A solution of compound **18** (358 mg, 1.7 mmol) in dry THF (3 mL) was added to a solution of LDA (3.4 mL, 6.8 mmol) in THF at -20 ^{o}C. The resulting deep orange solution was stirred at 0 ^{o}C for 2h and the precipitate that formed was dissolved by the addition of HMPA (0.3 mL, 1.7 mmol). To this orange solution, a solution of 4-bromobut-1-yne (0.18 mL, 1.9 mmol) in THF was added dropwise at -20 ^{o}C. The mixture was stirred at 0 ^{o}C for 2h and at 25 ^{o}C for 12h. The reaction was acidified with 3 M HCl, extracted with ether, washed with water, brine and dried with $MgSO_4$, filtered and concentrated under reduced pressure. The residue was purified by silica gel chromatography (pentane/EtOAc = 1:1) and afforded title compound (275 mg, 1.05 mmol, 62% yield). ^{1}H NMR (400 MHz, $CDCl_3$) δ 11.32 (br, 1H), 8.46 – 8.34 (m, 1H), 8.16 – 8.06 (m, 1H), 7.68 (d, *J* = 7.5 Hz, 1H), 7.57 – 7.51 (m, 2H), 7.43 (d, *J* = 7.6 Hz, 1H), 5.10 (t, *J* = 6.7 Hz, 1H), 4.66 – 4.62 (m, 2H), 4.53 (dd, *J* = 8.6, 6.1 Hz, 1H), 3.45 (s, 1H), 2.95 – 2.84 (m, 1H), 2.58 – 2.50 (m, 1H). ^{13}C NMR (101 MHz, $CDCl_3$) δ 179.64, 135.62, 133.98, 131.29, 130.89, 127.16, 126.88, 126.58, 124.41, 123.51, 119.97, 87.41, 82.64, 81.71, 76.30, 46.43, 31.27, 31.14.

(*E*)-6-(bromomethylene)-3-(4-ethynylnaphthalen-1-yl)tetrahydro-2*H*-pyran-2-one (12). To $KHCO_3$ (25 mg, 0.25 mmol) was added compound **19** (65 mg, 0.248 mmol) and DCM (3 mL) with stirring at r.t. After 10 mins, NBS (44 mg, 0.25 mmol) was added followed by addition of H_2O (18 µL, 0.99 mmol). The solution was then washed with 5% NaS_2O_3, water, brine and dried over $MgSO_4$, filtered and concentrated under reduced pressure. The residue was purified by silica gel chromatography (pentane/ EtOAc = 1%-10%) to afford title compound (8 mg, 0.023 mmol, 8% yield). ^{1}H NMR (400 MHz, $CDCl_3$) δ 8.24 – 8.13 (m, 1H), 8.03 – 7.96 (m, 1H), 7.76 – 7.71 (m, 1H), 7.63 – 7.55 (m, 2H), 7.49 (dd, *J* = 7.5, 2.5 Hz, 1H), 7.06 (s, 1H), 5.75 – 5.68 (m, 1H), 2.62 – 2.53 (m,

1H), 2.45 – 2.39 (m, 1H), 2.22 – 2.13 (m, 1H), 2.10 (d, *J* = 2.8 Hz, 1H), 2.07 – 1.96 (m, 1H). ^{13}C NMR (101 MHz, $CDCl_3$) δ 142.10, 134.84, 130.47, 129.67, 126.70, 126.58, 125.79, 123.60, 123.46, 122.45, 119.62, 106.78, 69.80, 69.48, 69.34, 36.76, 15.51.

(*E*)-3-(7-(4-(3-(4-(4-(6-(bromomethylene)-2-oxotetrahydro-2*H*-pyran-3-yl)naphthalen-1-yl)-1*H*-1,2,3-triazol-1-yl)propoxy)phenyl)-5,5-difluoro-1,3-dimethyl-5*H*-4l4,5l4-dipyrrolo[1,2-c:2',1'-f][1,3,2]diazaborinin-2-yl)propanoic acid (13) Compound **12** (6.0 mg, 0.018 mmol) and compound **20** (9.86 mg, 0.021 mmol) were dissolved in degassed DCM/H_2O (2 mL, 1:1, v/v) and aqueous solutions of sodium ascorbate (2.61 mg, 0.013 mmol) and $CuSO_4 \cdot 5H_2O$(2.20 mg, 8.79 µmol) (20%mol) were added. The resulting mixture was stirred vigorously for 2h, after which TLC indicated completed conversion of the reaction. The solvents were evaporated under reduced pressure, and the residue was taken up in DCM and purified by silica column chromatography (DCM/MeOH = 0.5%-5%). The pure final product was obtained (5.4 mg, 6.68 µmol, 38% yield). ^{1}H NMR (600 MHz, $CDCl_3$) δ 8.13 – 7.94 (m, 2H), 7.86 – 7.62 (m, 3H), 7.59 – 7.41 (m, 3H), 7.09 (s, 1H), 7.04 (s, 1H), 6.94 (d, *J* = 4.0 Hz, 1H), 6.89 (d, *J* = 8.1 Hz, 2H), 6.48 (dd, *J* = 6.6, 3.9 Hz, 1H), 5.60 (br, 1H), 4.83 – 4.39 (m, 2H), 4.03 – 3.87 (m, 2H), 2.74 (s, 2H), 2.51 – 2.45 (m, 6H), 2.21 (s, 4H), 1.29 – 1.22 (m, 5H). ^{13}C NMR (151 MHz, $CDCl_3$) δ 159.58, 159.23, 155.44, 140.06, 135.10, 134.65, 134.58, 134.48, 130.91, 130.65, 130.57, 129.98, 129.74, 129.70, 128.13, 126.91, 126.72, 126.54, 126.09, 126.08, 125.82, 123.18, 119.94, 119.90, 118.48, 114.24, 106.89, 106.79, 64.06, 54.00, 32.07, 29.85, 29.81, 29.52, 22.85, 14.29, 13.33, 9.82, 0.15.

References

1. Devane, W. A.; Hanus, L.; Breuer, A.; Pertwee, R. G.; Stevenson, L. A.; Griffin, G.; Gibson, D.; Mandelbaum, A.; Etinger, A.; Mechoulam, R. Isolation and structure of a brain constituent that binds to the cannabinoid receptor. *Science* **1992,** 258, 1946-1949.
2. Di Marzo, V. Endocannabinoid signaling in the brain: biosynthetic mechanisms in the limelight. *Nauture Neuroscience* **2011,** 14, 9-15.
3. Gaoni, Y.; Mechoulam, R. Isolation, structure, and partial synthesis of an active constituent of hashish. *Journal of the American Chemical Society* **1964,** 86, 1646-1647.
4. Di Marzo, V.; Bifulco, M.; De Petrocellis, L. The endocannabinoid system and its therapeutic exploitation. *Nature Reviews. Drug Discovery* **2004,** 3, 771-784.
5. Di Marzo, V.; Stella, N.; Zimmer, A. Endocannabinoid signalling and the deteriorating brain. *Nature Reviews Neuroscience* **2015,** 16, 30-42.
6. Lutz, B.; Marsicano, G.; Maldonado, R.; Hillard, C. J. The endocannabinoid system in guarding against fear, anxiety and stress. *Nature Reviews Neuroscience* **2015,** 16, 705-718.
7. Mendizabal, V. E.; Adler-Graschinsky, E. Cannabinoids as therapeutic agents in cardiovascular disease: a tale of passions and illusions. *British Journal Pharmacology* **2007,** 151, 427-440.
8. Parsons, L. H.; Hurd, Y. L. Endocannabinoid signalling in reward and addiction. *Nature Reviews Neuroscience* **2015,** 16, 579-594.

9. Di Marzo, V.; Matias, I. Endocannabinoid control of food intake and energy balance. *Nature Neuroscience* **2005,** 8, 585-589.
10. Moreira, F. A.; Crippa, J. A. S. The psychiatric side-effects of rimonabant. *Revista Brasileira de Psiquiatria* **2009,** 31, 145-153.
11. Van Gaal, L. F.; Rissanen, A. M.; Scheen, A. J.; Ziegler, O.; Rossner, S.; Group, R. I.-E. S. Effects of the cannabinoid-1 receptor blocker rimonabant on weight reduction and cardiovascular risk factors in overweight patients: 1-year experience from the RIO-Europe study. *Lancet* **2005,** 365, 1389-1397.
12. Di Marzo, V.; Fontana, A.; Cadas, H.; Schinelli, S.; Cimino, G.; Schwartz, J. C.; Piomelli, D. Formation and inactivation of endogenous cannabinoid anandamide in central neurons. *Nature* **1994,** 372, 686-91.
13. Iannotti, F. A.; Di Marzo, V.; Petrosino, S. Endocannabinoids and endocannabinoid-related mediators: Targets, metabolism and role in neurological disorders. *Progress in Lipid Research* **2016,** 62, 107-128.
14. Reisenberg, M.; Singh, P. K.; Williams, G.; Doherty, P. The diacylglycerol lipases: structure, regulation and roles in and beyond endocannabinoid signalling. *Philosophical transactions of the Royal Society of London. Series B, Biological sciences* **2012,** 367, 3264-3275.
15. Tanimura, A.; Yamazaki, M.; Hashimotodani, Y.; Uchigashima, M.; Kawata, S.; Abe, M.; Kita, Y.; Hashimoto, K.; Shimizu, T.; Watanabe, M.; Sakimura, K.; Kano, M. The endocannabinoid 2-arachidonoylglycerol produced by diacylglycerol lipase alpha mediates retrograde suppression of synaptic transmission. *Neuron* **2010,** 65, 320-327.
16. Gao, Y.; Vasilyev, D. V.; Goncalves, M. B.; Howell, F. V.; Hobbs, C.; Reisenberg, M.; Shen, R.; Zhang, M. Y.; Strassle, B. W.; Lu, P.; Mark, L.; Piesla, M. J.; Deng, K.; Kouranova, E. V.; Ring, R. H.; Whiteside, G. T.; Bates, B.; Walsh, F. S.; Williams, G.; Pangalos, M. N.; Samad, T. A.; Doherty, P. Loss of retrograde endocannabinoid signaling and reduced adult neurogenesis in diacylglycerol lipase knock-out mice. *The Journal of Neuroscience : the official Journal of the Society for Neuroscience* **2010,** 30, 2017-2024.
17. Powell, D. R.; Gay, J. P.; Wilganowski, N.; Doree, D.; Savelieva, K. V.; Lanthorn, T. H.; Read, R.; Vogel, P.; Hansen, G. M.; Brommage, R.; Ding, Z. M.; Desai, U.; Zambrowicz, B. Diacylglycerol lipase a knockout mice demonstrate metabolic and behavioral phenotypes similar to those of cannabinoid receptor 1 knockout mice. *Frontiers in Endocrinology* **2015,** 6.
18. Hsu, K. L.; Tsuboi, K.; Adibekian, A.; Pugh, H.; Masuda, K.; Cravatt, B. F. DAGLbeta inhibition perturbs a lipid network involved in macrophage inflammatory responses. *Nature Chemical Biology* **2012,** 8, 999-1007.
19. Kohnz, R. A.; Nomura, D. K. Chemical approaches to therapeutically target the metabolism and signaling of the endocannabinoid 2-AG and eicosanoids. *Chemical Society reviews* **2014,** 43, 6859-6869.
20. Bisogno, T.; Burston, J. J.; Rai, R.; Allara, M.; Saha, B.; Mahadevan, A.; Razdan, R. K.; Wiley, J. L.; Di Marzo, V. Synthesis and pharmacological activity of a potent inhibitor of the biosynthesis of the endocannabinoid 2-arachidonoylglycerol. *ChemMedChem* **2009,** 4, 946-950.
21. Di Marzo, V.; Goparaju, S. K.; Wang, L.; Liu, J.; Batkai, S.; Jarai, Z.; Fezza, F.; Miura, G. I.; Palmiter, R. D.; Sugiura, T.; Kunos, G. Leptin-regulated endocannabinoids are involved in maintaining food intake. *Nature* **2001,** 410, 822-825.

22. Fisette, A.; Tobin, S.; Decarie-Spain, L.; Bouyakdan, K.; Peyot, M. L.; Madiraju, S. R.; Prentki, M.; Fulton, S.; Alquier, T. alpha/beta-Hydrolase domain 6 in the ventromedial hypothalamus controls energy metabolism flexibility. *Cell Reports* **2016,** 17, 1217-1226.
23. Tchantchou, F.; Zhang, Y. M. Selective Inhibition of alpha/beta-Hydrolase domain 6 attenuates neurodegeneration, alleviates blood brain barrier breakdown, and improves functional recovery in a mouse model of traumatic brain injury. *Journal of Neurotrauma* **2013,** 30, 565-579.
24. Nomura, D. K.; Long, J. Z.; Niessen, S.; Hoover, H. S.; Ng, S. W.; Cravatt, B. F. Monoacylglycerol lipase regulates a fatty acid network that promotes cancer pathogenesis. *Cell* **2010,** 140, 49-61.
25. Ahn, K.; McKinney, M. K.; Cravatt, B. F. Enzymatic pathways that regulate endocannabinoid signaling in the nervous system. *Chemical Reviews* **2008,** 108, 1687-1707.
26. Jin, X. H.; Okamoto, Y.; Morishita, J.; Tsuboi, K.; Tonai, T.; Ueda, N. Discovery and characterization of a Ca2+-independent phosphatidylethanolamine N-acyltransferase generating the anandamide precursor and its congeners. *The Journal of Biological Chemistry* **2007,** 282, 3614-3623.
27. Ogura, Y.; Parsons, W. H.; Kamat, S. S.; Cravatt, B. F. A calcium-dependent acyltransferase that produces N-acyl phosphatidylethanolamines. *Nature Chemical Biology* **2016,** 12, 669-671.
28. Cadas, H.; diTomaso, E.; Piomelli, D. Occurrence and biosynthesis of endogenous cannabinoid precursor, N-arachidonoyl phosphatidylethanolamine, in rat brain. *Journal of Neuroscience* **1997,** 17, 1226-1242.